

Enhanced field emission properties of indium-doped ZnO nanorods

M.N. Jung^{a,g}, J.E. Koo^a, G.S. Kil^b, S.H. Park^c, W.J. Lee^d, D.C. Oh^e, H.J. Lee^f and J.H. Chang^{a,*}

^aDepartment of Nano-semiconductor Engineering, National Korea Maritime Univ., Busan, 606-791, Korea

^bDivision of Electrical and Electronics Engineering, National Korea Maritime Univ., Busan, 606-791, Korea

^cNational Institute for Materials Science, Tsukuba, 305-0044, Japan

^dElectronic Ceramics Center, Dong Eui Univ., Busan, 614-714, Korea

^eDep. of Defense Science & Technology, Hoseo Univ., Asan, 336-795, Korea

^fCenter for Interdisciplinary Research, Tohoku Univ., Sendai, 980-8578, Japan

^gInstitute for Materials Research, Tohoku University, Sendai 980-8578, Japan

Various group-III metal (Al, Ga, and In)-doped ZnO nanorods were synthesized by a vapor phase deposition in a horizontal reactor. The morphology and optical properties of the group-III metal doped nanorods were compared to determine the best candidate as a donor impurity. Among these three nanorod samples, indium-doped ZnO (ZnO : In) nanorods revealed the best result in terms of uniform morphology, strong luminescence intensity and negligible deep levels. The electrical properties of ZnO:In nanorods with various In-composition were indirectly assessed by Hall-effect measurements of the wetting layer. Also, we found that the ZnO : In nanorods show considerably improved field emission properties in compared to undoped ZnO nanorods with a low threshold electric field (E_{th}) of 4.32 V/ μ m at a current density of 0.1 μ A/cm² and a high field enhancement factor of 1258.

Key words: Oxides, Vapor deposition, Electron microscopy, Electrical properties.

Introduction

There have been many studies on the synthesis and their applications of various ZnO nanostructures [1-2]. From the viewpoint of applications, one-dimensional (1D) ZnO nanorods have the advantage of a simple geometry [3-4]. However, the realization of devices based on 1D ZnO nanorods depends on obtaining high-quality nanorods with a controlled morphology. To widen the application of ZnO nanorods, conductivity control is an important issue to be investigated further. Note that a doping concentration of 10^{18} cm⁻³ means one dopant atom in 10 nm³, any fluctuation of dopant distribution will result in totally different device functionality. Thus, it should be kept in mind that the choice of an effective dopant is important in order to avoid the degradation of devices caused by the presence of impurities. However, to realize n-type ZnO nanorods, comparative research on the proper dopants for the realization of n-type ZnO nanorods under consistent growth conditions has not yet taken place.

Recently, Bae *et al.* reported on the comparative structure and optical properties of Ga-, In, and Sn-doped ZnO nanowires synthesized via thermal evaporation [5]. They showed that the average content for doped ZnO nanowires grown at a high growth temperature (800-1000 °C) was

as high as about 15% for all three dopants. However, with respect to the synthesis of n-type ZnO nanorods, there has been few comparative research studies to establish the proper dopant.

This paper focuses on group-III metal doped ZnO (ZnO : M; M = Al, Ga, and In) nanorods grown by the vertical vapor phase transportation (V-VPT) method. The paper gives the results of the structure and optical properties of ZnO : M nanorods. Finally, we present field emission measurements performed using ZnO : M nanorods with excellent properties both structurally and optically.

Experimental

ZnO : M nanorods were grown on AuGe/Si (111) substrates by the V-VPT method in a horizontal reactor. In order to grow the ZnO : M nanorods, we prepared various dopant sources (Ga₂O₃, Al, and In). These dopants were mixed with Zn powder (average particle size = 150 μ m, quantity ~0.05 g) to grow doped nanorods. We varied the weight ratio ($R_W = W_D / (W_D + W_{Zn})$, W_D and W_{Zn} being the weight of dopant and Zn sources, respectively). Since each dopant element has a considerably different evaporation pressure, we had to vary the formation temperature in order to grow doped-ZnO nanorods. The growth temperature for In (ZnO : In) and Al (ZnO : Al) doped ZnO was 600 °C under an Ar gas flow of 600 sccm. For the synthesis of Ga (ZnO : Ga) doped ZnO nanorods, we selected not Ga powder but Ga₂O₃ powder because of an excessively

*Corresponding author:

Tel : +82-51-410-4783

Fax: +82-41-410-3986

E-mail: jiho_chang@hhu.ac.kr

large mesh of Ga powder ($> 850 \mu\text{m}$). Thus, the growth temperature was as high as 1100°C . The morphology of each sample was observed by a field emission scanning electron microscope (FE-SEM). The crystallinity of the samples was investigated by photoluminescence (PL) at room temperature with a He-Cd laser (325 nm) as an excitation source. Furthermore, conductivity (σ), carrier concentration (n), and mobility (μ) of the wetting layers were estimated using the Hall effect with a van der Pauw configuration to estimate the carrier concentration in the doped ZnO nanorods. Finally field emission measurements were carried out in a vacuum under $10^{-5} \mu\text{Pa}$ at room temperature. Indium tin oxide (ITO) glass was used as an anode and the nominal distance between the cathode and anode was $200 \mu\text{m}$. The current was measured by varying the applied voltage between the cathode and anode from 0 to 1400 V with a 10 V step.

Results and Discussion

The physical properties of various dopants are summarized in Table 1. It shows that metal-powders and metal-oxides (M_2O_3) sources have a fairly low vapor pressure within the reported growth temperature range for ZnO nanorods ($600\text{-}1000^\circ\text{C}$). Among these group-III metals, In has a relatively high vapor pressure in comparison with Ga or Al. Furthermore, the Mott density of In in ZnO is known to be as low as $4 \times 10^{18} \text{ cm}^{-3}$ [6] which indicates that a rapid metallic transition of ZnO could be achieved by In-incorporation.

Fig. 1 shows the SEM images of (a) ZnO, (b) ZnO : Ga, (c-d) ZnO : Al and (e-f) ZnO : In nanostructures. ZnO nanorods (Fig. 1(a)) have a uniform diameter of $60\text{-}70 \text{ nm}$ with a length of approximately $4 \mu\text{m}$. Fig. 1(b) shows ZnO : Ga nanofibers ($R_W = 0.5$ with graphite = 0.05 g) $0.8\text{-}1.2 \mu\text{m}$ -long and $150\text{-}250 \text{ nm}$ -thick, which are very similar to those previously reported [7]. Fig. 1(c)-(d) shows ZnO : Al nanorods grown with $R_W = 0.25$ and 0.5 . When we increased the R_W , we observed an increase in diameter from 125 nm to 150 nm and a decrease in length from

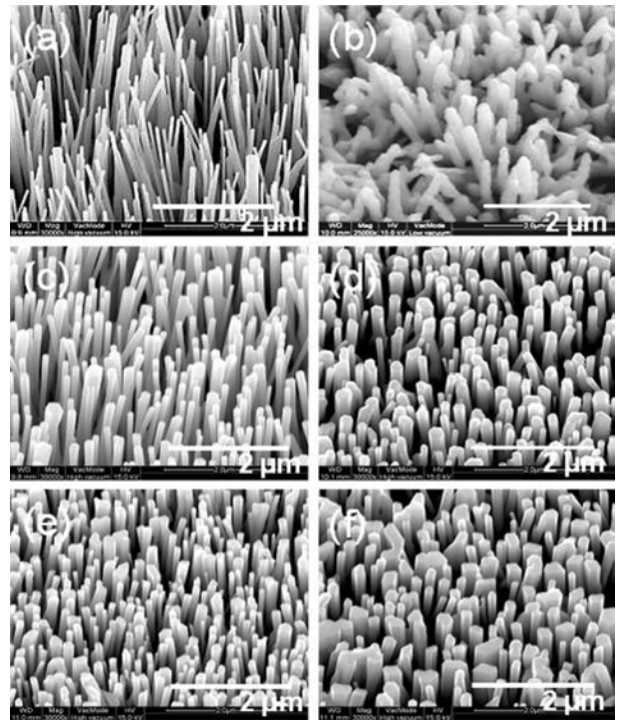


Fig. 1. SEM images of (a) ZnO nanorods using only a Zn source (0.05 g) at 600°C , (b) ZnO : Ga nanorods at a weight ratio ($R_W = \text{Ga}_2O_3/[\text{Ga}_2O_3 + \text{Zn}]$) of 0.5 at 1100°C . The amount of graphite was 0.05 g , (c-d) ZnO : Al nanorods grown at R_W ($R_W = \text{Al}/[\text{Al} + \text{Zn}]$) of 0.25 and 0.5 at 600°C , respectively. (e-f) ZnO : In nanorods grown at R_W ($R_W = \text{In}/[\text{In} + \text{Zn}]$) of 0.08 and 0.14 at 600°C .

$2.5 \mu\text{m}$ to $1.9 \mu\text{m}$. Similarly, ZnO : In nanorods ($R_W = 0.08$ and 0.14), Fig. 1(e)-(f), show a diameter of 147 nm with a length of $1.2 \mu\text{m}$ ($R_W = 0.08$), 190 nm -thick and $0.9 \mu\text{m}$ -long legs ($R_W = 0.14$). In the case of the nanostructure of ZnO : Ga, various problems remain in terms of the morphological control of the nanostructure. Ga segregates easily, which results in a non-uniform vapor pressure of Ga. This hinders obtaining uniform nanostructures, although the addition of graphite helps to prevent the non-uniform vapor pressure of Ga.

Fig. 2 shows the PL spectra at room temperature of ZnO, ZnO : Ga ($R_W = 0.5$ with graphite = 0.005 g), ZnO : Al ($R_W = 0.25$) and ZnO : In ($R_W = 0.08$) nanorods. In Fig. 2 the ZnO nanorods reveal a sharp near-band-edge (NBE) peak at 3.236 eV in the ultraviolet (UV) region. In the ZnO : M samples, NBE peak shifts can be observed. It is useful to consider the NBE emission position in terms of the theory of a semiconductor-metal transition. It is well known that the NBE emission position blue-shifts when the impurity concentration is kept under the Mott critical density, while it red-shifts abruptly when the Mott transition occurred. Hence, the red-shifts of the NBE emission are attributed to a high concentration (presumably higher than the Mott density) of impurity atoms in the nanorods. The inset in Fig. 2 shows a full width at half maximum (FWHM) and PL integrated intensity ratio of the NBE emissions to the deep level emissions ($I_{\text{NBE}}/I_{\text{Deep}}$) for each

Table 1. Physical properties of various ZnO : M ($M = \text{Al}$, Ga , and In) and M_2O_3

Materials	Melting point ($^\circ\text{C}$)	Crystal structure	Vapor pressure at 1 Pa ($^\circ\text{C}$)	Mott density (cm^{-3})
Zn	419	Hexagonal	337	-
ZnO	1975	Hexagonal		$4 \times 10^{18} [15]$
Al, (ZnO : Al)	660	Cubic	1219	$(4.5 \times 10^{20} [16])$
Al_2O_3	2044	Octahedral	-	-
Ga, (ZnO : Ga)	29.8	Orthorhombic	1037	$(4 \times 10^{20} [17])$
Ga_2O_3	1780	Monoclinic	-	-
In, (ZnO : In)	156.6	Tetragonal	923	$(4 \times 10^{19} [6])$
In_2O_3	1910	Cubic	-	-

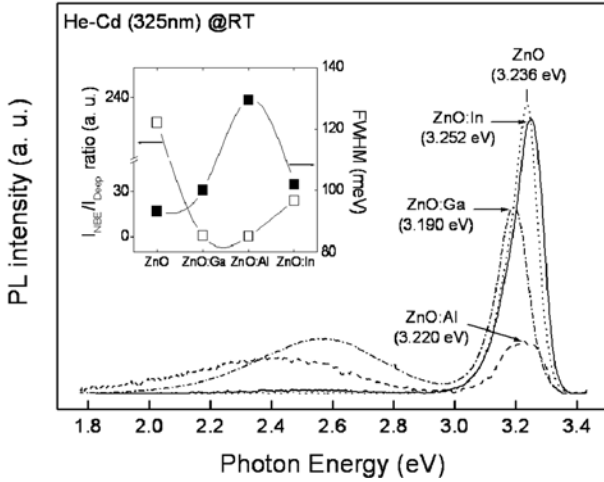


Fig. 2. PL spectra of ZnO : M at room temperature.

sample. Note that the FWHM of the NBE emissions in our samples are considerably narrower than the reported values for ZnO nanorods (175 meV), ZnO : In nanorods (179 meV) [8], and ZnO : Al nanorods grown by various methods [9]. Although our samples show relatively good luminescence properties, the ZnO : Al nanorods revealed a considerable FWHM broadening with the lowest $I_{\text{NBE}}/I_{\text{Deep}}$ ratio. It should be noted that degradation of luminescence properties, in other words the broadening of the PL band with increasing Al-content and a decrease of luminescence intensity, has usually been reported from ZnO : Al film [9]. The reason might be explained in terms of the strongest oxidation tendency of Al atom among the tested group-III metals, which will hinder a uniform distribution of Al-atoms in the ZnO host crystal.

Nevertheless, further investigation into the crystallinity of nanorods and careful consideration is required before determining the most appropriate dopant for specific applications, the SEM (Fig. 1) and PL results (Fig. 2) made us decide on indium as a dopant for ZnO nanorods grown by V-VPT. Therefore ZnO : In nanorods with various In-content were prepared to study the effect of external carrier concentration increases.

We tried Hall effect measurements using a wetting layer for a quantitative discussion on the increase of extrinsic carrier concentration in ZnO : In nanorods. Hall effect measurements were performed by using a wetting layer (with thickness H) of the ZnO : In_x samples instead of preparing a film deposited under the similar growth conditions [10], because usually there are substantial differences.

Fig. 3 shows the carrier concentration (n), mobility (μ), and conductivity (σ) of the wetting layers of ZnO : In ($R_w = 0, 0.08$, and 0.14) samples measured by the Hall effect. Fig. 3 shows that the carrier concentration n increases up to $2.89 \times 10^{19} \text{ cm}^{-3}$ ($\mu = 103 \text{ cm}^2 \text{V}^{-1} \cdot \text{s}^{-1}$) for the ZnO : In ($R_w = 0.08$) sample and continuously increases to $8.88 \times 10^{20} \text{ cm}^{-3}$ ($\mu = 85.4 \text{ cm}^2 \text{V}^{-1} \cdot \text{s}^{-1}$) for ZnO : In ($R_w = 0.14$) sample. The increased In-concentration is entirely dependent on the carrier concentration of the sample. Moreover, note

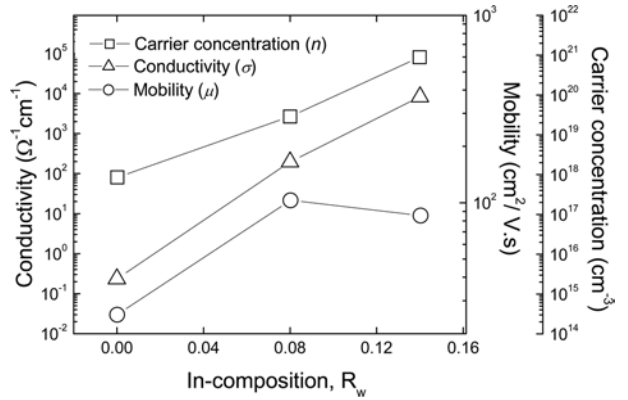


Fig. 3. Carrier concentration (n), mobility (μ), and conductivity (σ) of the wetting layers for ZnO and ZnO : In ($R_w = 0, 0.08$, and 0.14) nanorods.

that the carrier concentration (especially for ZnO : In with $R_w = 0.14$) is much higher than the reported Mott density of $4 \times 10^{19} \text{ cm}^{-3}$ which has been reported from ZnO : In films [6].

We consider that the mobility is also closely related with the level of In-concentration. It seems to be determined by at least two dominant factors. One is the increase of grain size [11] and the other is scattering caused by ionized impurities. The grain size of a wetting layer is defined as the characteristic diameter (D^*) in ref. [12], which shows the D^* value increases with an increase in the In-content of the sample, and the grain size increases but ionized impurity scattering reduces carrier mobility. Therefore, the mobility increases up to $103 \text{ cm}^2 \text{V}^{-1} \cdot \text{s}^{-1}$ for the ZnO : In ($R_w = 0.08$) sample with increasing D^* , but decreases due to the increase in ionized impurity density for the ZnO : In ($R_w = 0.14$) sample. These results clearly indicate that In-doping considerably increases the carrier concentration of the wetting layer. Hence, we tentatively assumed that the In-content in ZnO : In nanorods also increases by In-doping. If this assumption is valid, the minimum electric field for field emission from ZnO : In nanorods should be lower than the ZnO nanorods.

Generally, a fine nanostructure is a critical requirement for the development of field emission devices, since a fine nanostructure enhances the field enhancement factor (β) [13, 14], which reflects the ability of emitters to enhance the local electric field at the tip. From this point of view, we could expect an increase of the threshold electric field (E_{th}) from ZnO : In nanorods, despite the increase in conductivity. However, the work function (ϕ) might be expected to show the opposite effect. If the reduction of ϕ dominates the emission efficiency, the E_{th} will be reduced by increasing the In-composition. This would also be clear evidence of ϕ control by impurity doping in nanocrystals.

Fig. 4 shows field emission properties of ZnO : In nanorods ($R_w = 0, 0.08$, and 0.14). The E_{th} is defined as the E corresponding to the J of $0.1 \mu\text{A}/\text{cm}^2$. The E_{th} and β values are shown in the inset of Fig. 4. The respective E_{th} of ZnO, ZnO : In ($R_w = 0.08$), and ZnO : In ($R_w = 0.14$)

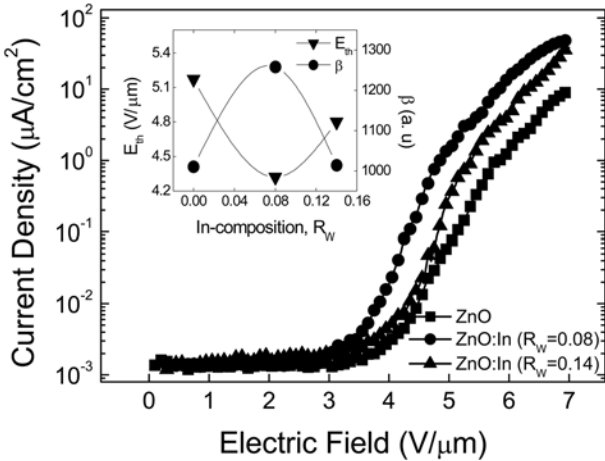


Fig. 4. Field emission properties of ZnO and ZnO : In ($R_w = 0$, 0.08, and 0.14) nanorods.

nanorods are estimated to be 5.17, 4.32, and 4.82 V/ μ m. The ZnO : In nanorods show relatively low E_{th} . In the case of the ZnO : In nanorods with $R_w = 0.08$, the calculated β value of 1258 is much higher than for the other samples. As discussed above, these results are only obtained when the effect of ϕ reduction more than compensates for the increase of β , and it strongly indicates the reduction in ϕ of ZnO nanostructures by In doping.

Conclusions

Various group-III elements doped ZnO nanorods were synthesized by V-VPT. It was particularly noted that the ZnO : In nanorods ($R_w = 0.08$) had a uniform morphology and an excellent luminescence property compared with other samples. By increasing the In-content, the carrier concentration and conductivity of the wetting layer of ZnO : In samples were increased, forming ZnO : In nanorods with a $R_w = 0.08$ low threshold electric field (E_{th}) of 4.32 V/ μ m at a current density of 0.1 μ A/cm² with a high field enhancement factor of 1258, which in turn implies a decrease of the work function by In-incorporation.

Acknowledgments

This research was supported by the MKE(the Ministry of Knowledge Economy), Korea, under the ITRC(Information Technology Research Center) support program supervised by the NIPA(National IT Industry Promotion Agency)(NIPA-2010-C1090-1021-0015).

References

1. S. Fan, M.G. Chapline, N.R. Franklin, T.W. Tombler, A.M. Cassell and H. Dai, Science 283 (1999) 512-514.
2. Z.F. Ren, Z.P. Huang, J.W. Xu, J.H. Wang, P. Bush, M.P. Siegal and P.N. Rovencio, Science 282 (1997) 1105-1107.
3. M.H. Huang, S. Mao, H. Feick, H.Q. Yan, Y.Y. Wu, H. Kind, E. Weber, R. Russo and P.D. Yang, Science 292 (2001) 1897-1899.
4. Q. Wan, Q.H. Li, Y.J. Chen, T.H. Wang X.L. He, J.P. Li and C.L. Lin, Appl. Phys. Lett. 84 (2004) 3654-3656.
5. S.Y. Bae, C.W. Na, J.H. Kang and J.H. Park, J. Phys. Chem. B 109 (2005) 2526-2531.
6. K.J. Kim and Y.R. Park, Appl. Phys. Lett. 78 (2001) 475-477.
7. C.X. Xu, X.W. Sun and B.J. Chen, Appl. Phys. Lett. 84 (2004) 1540-1542.
8. Y.W. Chen, Y.C. Liu, S.X. Lu, C.S. Xu, C.L. Shao, C. Wang, J.Y. Zhang, Y.M. Lu, D.Z. Shen and X.W. Fan, J. Chem. Phys. 123 (2005) 134701-134705.
9. X. Wang, G. Li and Y. Wang, Chem. Phys. Lett. 469 (2009) 308-312.
10. C.X. Xu, X.W. Sun and B.J. Chen, Appl. Phys. Lett. 84 (2004) 1540-1542.
11. D.H. Zhang and H.L. Ma, Appl. Phys. A: Mater. Sci. Process. 62 (1996) 487-492.
12. M.N. Jung, J.E. Koo, S.J. Oh, B.W. Lee, W.J. Lee, S.H. Ha, Y.R. Cho and J.H. Chang, Appl. Phys. Lett. 94 (2009) 041906-041908.
13. Y.W. Zhu, H.Z. Zhang, X.C. Sun, S.Q. Feng, J. Xu, Q. Zhao, B. Xiang, R.M. Wang and D.P. Yu, Appl. Phys. Lett. 83 (2003) 144-146.
14. Q. Zhao, H.Z. Zhang, Y.W. Zhu, S.Q. Feng, X.C. Sun, J. Xu and D.P. Yu, Appl. Phys. Lett. 86 (2005) 203115-203117.
15. C. Klingshirn, Phys. Stat. Sol. (b) 244 (2007) 3027-3073.
16. B.E. Sernelius, K.-F. Berggren, Z.-C. Jin, I. Hamberg and C.G. Granqvist, Phys. Rev. B 37 (1988) 10244-10248.
17. J. Hu and R.G. Gordon, J. Appl. Phys. 72 (1992) 538-5392.